ARTICLE

Supramolecular Chemistry on Water-Soluble Carbon Nanotubes for Drug Loading and Delivery

Zhuang Liu, Xiaoming Sun, Nozomi Nakayama-Ratchford, and Hongjie Dai*

Department of Chemistry, Stanford University, Stanford, California 94305

ABSTRACT We show that large surface areas exist for supramolecular chemistry on single-walled carbon nanotubes (SWNTs) prefunctionalized noncovalently or covalently by common surfactant or acid-oxidation routes. Water-soluble SWNTs with poly(ethylene glycol) (PEG) functionalization *via* these routes allow for surprisingly high degrees of π-stacking of aromatic molecules, including a cancer drug (doxorubicin) with ultrahigh loading capacity, a widely used fluorescence molecule (fluorescein), and combinations of molecules. Binding of molecules to nanotubes and their release can be controlled by varying the pH. The strength of π-stacking of aromatic molecules is dependent on nanotube diameter, leading to a method for controlling the release rate of molecules from SWNTs by using nanotube materials with suitable diameter. This work introduces the concept of "functionalization partitioning" of SWNTs, *i.e.*, imparting multiple chemical species, such as PEG, drugs, and fluorescent tags, with different functionalities onto the surface of the same nanotube. Such chemical partitioning should open up new opportunities in chemical, biological, and medical applications of novel nanomaterials.

KEYWORDS: carbon nanotubes · functionalization · doxorubicin · supramolecular chemistry · drug delivery

Single-walled carbon nanotubes (SWNTs) are novel polyaromatic molecules with ultrahigh surface areas up to ~2600 m^2/g. The sidewall surface of a pristine SWNT is highly hydrophobic, and a major goal in carbon nanotube chemistry has been functionalization for aqueous solubility, aimed at exploiting nanotubes as macromolecules for chemistry, biology, and medicine.[1–12] While sidewall functionalization has been actively pursued,[1–5] little has been done to partition nanotube surfaces chemically for attaching various species to facilitate basic and practical applications in chemistry, biology, and medicine.[6–10,12–14] For potential drug delivery applications, efficient *in vivo* tumor accumulation of SWNTs in mice has been achieved by conjugating a cyclic arginine–glycine–aspartic acid (RGD) peptide to water-soluble SWNTs functionalized with poly(ethylene glycol) (PEG). Thus far, little has been done to devise rational strategies for attaching drug molecules onto nanotubes, especially together with targeting or homing moieties for targeted drug delivery for disease treatment.

Surfactant adsorption[5] and covalent oxidation[4] by acid reflux[15,16] have been the most widely used functionalization schemes, with PEG chains added to enable solubility in salt and biological solutions.[12,17] Thus far, further chemical reactions with functionalized SWNTs have relied on covalent linkage of molecules to terminal functional groups imparted onto nanotubes.[7] Here, we show that much room exists for carrying out supramolecular chemistry[18] assembly of molecules on SWNTs prefunctionalized noncovalently or covalently by common surfactant or acid-oxidation routes. Aqueous soluble SWNTs with PEG functionalization by these routes allow for π-stacking of various aromatic molecules, including a cancer chemotherapy drug (doxorubicin) with an ultrahigh loading capacity of ~400% by weight and a widely used fluorescence molecule (fluorescein). Binding of molecules to nanotubes and their release exhibit novel diameter dependence and can be controlled by varying the pH. These results uncover exciting opportunities for supramolecular chemistry on water-soluble SWNTs as a promising way of attaching drugs to nanotube vehicles, for applications ranging from drug delivery to chemical and biological imaging and sensing.

RESULTS AND DISCUSSION

Doxorubicin Loading on PEGylated SWNTs. Our starting materials were aqueous solutions of high-pressure CO decomposition (Hipco) SWNTs (mean diameter ~1.3 nm and length ~200 nm) functionalized noncovalently by a surfactant [phospholipid (PL)-

*Address correspondence to hdai@stanford.edu.

Received for review May 22, 2007 and accepted June 22, 2007.

Published online August 14, 2007.
10.1021/nn700040t CCC: $37.00

PEG, ~120 poly(ethylene oxide) (PEO)units][7,12] or covalently by PEGylation (~220 PEO units) of –COOH groups on oxidized SWNTs generated by refluxing[15,16] in 2.6 M nitric acid. After simple mixing of the SWNT solution with doxorubicin (DOX) at pH 9 overnight and then repeated filtering to remove free, unbound DOX in solution, we observed the formation of bound SWNT-DOX complexes for both phospholipid (PL-PEG-SWNT) and oxidized SWNTs (PEG-OXNT) (Figure 1a; Supporting Information, Figure S1), evidenced by the reddish color of the SWNT-DOX solutions due to adsorbed DOX and its characteristic UV–vis absorbance peak at 490 nm on top of the characteristic SWNT absorption spectrum (Figure 1b). Note that free, unbound DOX in the SWNT solution was removed thoroughly by repeated filtrations with a 100 kD molecular cutoff to retain only the SWNT-DOX complex. Further, the DOX-loaded SWNTs were stable in water and pH 7.4 physiological buffers, without any detectable release over hours. This was evidenced by filtering the SWNT-DOX solution at various time points after formation of the complex, with negligible amount of free DOX detected in the filtrate.

On the basis of optical absorbance data and molar extinction coefficients of DOX and SWNTs, we estimated ~50 DOX molecules bound to each 10 nm length of SWNTs, corresponding to a high weight ratio of ~4:1 between DOX and nanotubes. Radiolabeling was used to estimate the number of PEG functionalizations (on both PL-PEG-SWNT and PEG-OXNT) to be ~3 per 10 nm of SWNT length (Supporting Information, Table S1). This suggested that ~10% of the SWNT surface area was occupied by phospholipid molecules with extended PEG chains, while ~70–80% was complexed with DOX (Supporting Information, Figure S2, Table S1). Similar degrees of PEGylation and DOX loading were observed with PEG-OXNT. It was shown that a certain coverage of PEG chains on nanotubes was both necessary and sufficient to impart aqueous solubility of SWNTs without aggregation (especially for stability in high salt solutions and biological solutions such as serum;[12] Supporting Information, Figure S3); our results here suggested that unoccupied surface areas on functionalized SWNTs were useful for binding of other molecules. We suggest that noncovalent binding of DOX on SWNTs most likely occurred *via* π-stacking[6] and hydrophobic interactions due to the aromatic nature of the DOX molecule and the relatively low solubility of deprotonated DOX at basic conditions. Free, unbound DOX exhibited high fluorescence, while weak fluorescence was observed for DOX after binding to SWNTs (Figure 1c). This high degree of fluorescence quenching is evidence of π-stacked DOX, similar to other aromatic molecules π-stacked onto nanotubes.[19,20] Notably, SWNTs were observed to increase in average diameter when imaged by atomic force microscopy (AFM) after DOX loading and deposition onto a substrate

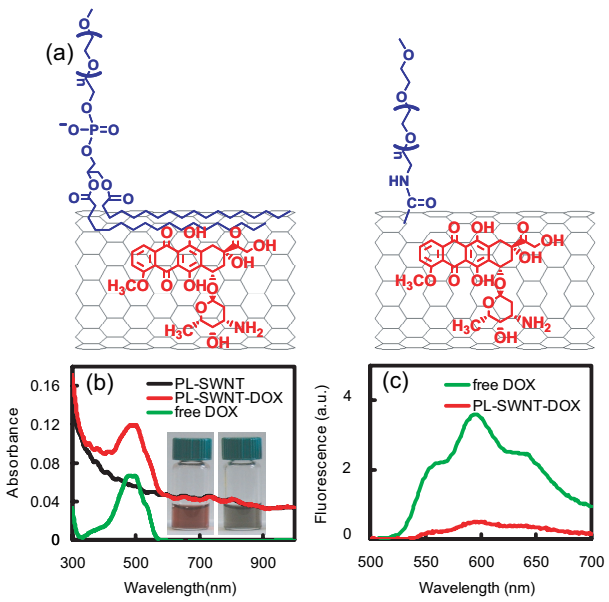

Figure 1. Supramolecular assembly of molecules on functionalized nanotubes. (a) Schematic drawings of doxorubicin π-stacking onto a nanotube prefunctionalized noncovalently by phospholipid (PL)-PEG (left) and covalently by PEGylation of a sidewall –COOH group (right), respectively. (b) UV–vis–NIR absorbance spectra of solutions of free doxorubicin (green), SWNTs with PL-PEG functionalization (black), and PL-PEG-SWNTs complexed with doxorubicin (red) after simple inculation in a doxorubicin solution at pH 9. Unbound doxorubicin was thoroughly filtered and washed away from the solution. The absorption peak at 490 nm was due to doxorubicin π-stacked on SWNTs, which was used for analyzing the amount of molecules loaded onto the nanotubes. Inset: Photo of SWNT solutions with and without bound doxorubicin. (c) Fluorescence spectra of solutions of free doxorubicin (green) and doxorubicin bound to SWNTs with PL-PEG functionalization (excitation at 488 nm) with the same doxorubicin concentration. Significant fluorescence quenching was evident for doxorubicin bound to SWNTs.

(Supporting Information, Figure S1). These data all suggest doxorubicin π-stacking onto unoccupied surface areas of PEG-SWNTs, forming a forest (PEG)–scrub (DOX) structure on SWNTs. This represents a novel partition and utilization of the SWNT sidewall surface area, affording a simple and interesting way to attach drugs to nanomaterials in a manner unique to carbon nanotubes, owing to the extended polyaromatic sidewalls. Notably, in control experiments, we found that DOX alone was incapable of solubilizing pristine SWNTs in water, and we did not find DOX replacing phospholipid molecules on SWNTs to any significant degree (Supporting Information, Figure S4).

pH-Dependent Doxorubicin Loading and Release from SWNTs. We found that the amount of doxorubicin bound onto SWNTs was pH-dependent, decreasing from a loading factor of ~4 (defined as DOX/SWNT weight ratio ~4) to ~2 and ~0.5 as pH was reduced from 9 to 7 and 5, respectively (Figure 2a–c). This trend was attributed to the increased hydrophilicity and higher solubility of DOX at lower pH caused by increased protonation of $-NH_2$ groups on DOX, thereby reducing the hydrophobic interaction between DOX and SWNTs. In terms of release, we found that DOX stacked on SWNTs remained

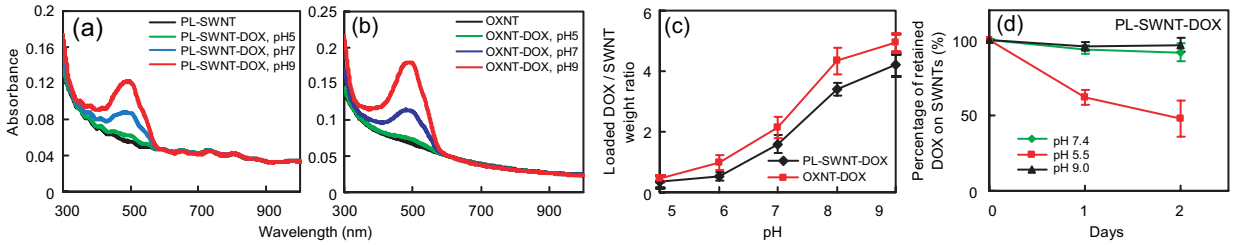

Figure 2. pH-dependent supramolecular loading of doxorubicin on noncovalent and covalently PEGylated SWNTs. (a,b) UV–vis–NIR absorbance spectra of (a) PL-PEG-functionalized Hipco SWNTs and (b) PEGylated nitric acid-oxidized SWNTs, with and without doxorubicin loaded at different pH values, as indicated. (c) Doxorubicin loading efficiency at various pH values for the two types of SWNTs. (d) Doxorubicin retained on PL-PEG-SWNTs over time in buffers at the three pH values indicated.

stably bound in basic buffer solutions, physiological buffers, and serum at pH 7.4 (Figure 2d; Supporting Information, Figures S5 and S6) at room temperature. In an acidic solution of pH 5.5, we observed appreciable release of DOX from Hipco SWNTs by ~40% over 1 day (Figure 2d; Supporting Information, Figure S6), attributed to the increased hydrophilicity and solubility of DOX at this pH. The pH-dependent drug release from SWNTs could be exploited for drug delivery applications since the micro-environments of extracellular tissues of tumors and intracellular lysosomes and endosomes are acidic, potentially facilitating active drug release from SWNT delivery vehicles.

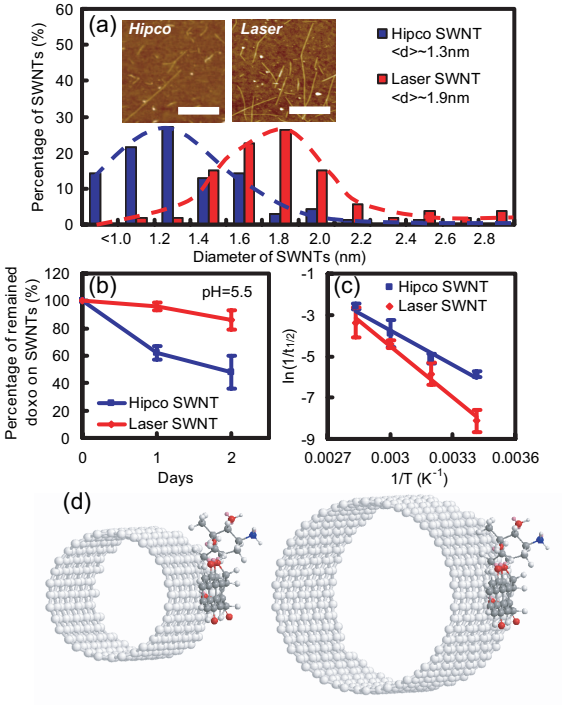

Figure 3. Supramolecular loading of aromatic drugs on nanotubes depends on nanotube diameter. (a) Diameter distributions of SWNTs in Hipco and laser-ablation materials. Inset: Atomic force microscopy (AFM) images of SWNTs in the two types of materials. The scale bar represents 200 nm. The diameter distributions were obtained by AFM topographic height measurements of ~100 PL-PEG-functionalized nanotubes in each material, after depositing them on Si substrates from solutions, followed by calcination at 350 °C to remove molecular coating. (b) Doxorubicin release curves (see Materials and Experiments) from Hipco SWNTs and laser-ablation SWNTs at an acidic pH of 5.5. A slower release rate was observed from larger diameter laser-ablation SWNTs. (c) Half-life, $t_{1/2}$ (*i.e.*, time needed for 50% molecular detachment), of doxorubicin on PL-PEG-functionalized Hipco and laser-ablation SWNTs respectively at various temperatures from 20 to 80 °C at pH 7.4. Solid lines are Arrhenius fits of $1/t_{1/2}(T) = A \exp(-E_B/k_BT)$ for extracting the desorption energy, E_B, of DOX from Hipco and laser-ablation nanotubes at pH 7.4. The half life $t_{1/2}$ was extracted by fitting DOX release *vs* time to an exponential decay function (Supporting Information, Figure S7). (d) Schematic drawings that show more favorable π-stacking of doxorubicin on a larger nanotube than on a smaller one.

Diameter-Dependent Doxorubicin Binding and Release from SWNTs. When using laser-ablation-grown SWNTs of larger diameter (mean $d \approx 1.9$ nm) than Hipco material ($d \approx 1.3$ nm) (Figure 3a), we observed obviously slower release of DOX (at the same pH, 5.5) than from Hipco tubes (Figure 3b). We heated the SWNT-DOX solutions to measure temperature-dependent release rate and half-life, $t_{1/2}$ (Figure 3c; Supporting Information, Figure S7), and found shorter $t_{1/2}$ or more rapid DOX release from SWNT surfaces at higher temperatures. We estimated ~48 and ~59 kJ/mol binding energies for DOX on Hipco and laser-ablation SWNTs (at pH 7.4), respectively (Supporting Information, Figure S7). This difference was rationalized by stronger π-stacking of aromatic molecules onto larger tubes with flatter graphitic sidewalls (Figure 3d). Thus, by choosing SWNTs of a specific diameter, one can tailor the molecular binding strength on SWNTs to vary the release rate and suit different applications.

***In Vitro* Toxicity Test of Doxorubicin-Loaded SWNTs.** Doxorubicin is a widely used chemotherapy drug for treating various cancers. While SWNTs without any DOX loading (PL-SWNT) exhibited no toxic effect on cells,[11] DOX-loaded SWNTs (PL-SWNT-DOX) induced significant U87 cancer cell death and cell apoptosis, similar to free DOX at a DOX concentration of 10 μM (Figure 4a–d), although the IC_{50} (half-maximum inhibitory concentration) value for PL-SWNT-DOX (~8 μM) was higher than that of free DOX (~2 μM) (Figure 4e). We suggest that DOX-loaded SWNTs were transported inside cells by nanotube transporters *via* endocytosis.[21] One of the potential advantages of using SWNTs as a drug carrier compared to free drug alone is the ability to target delivery for selective destruction of certain types of cells, reducing the toxicity to nontargeted cells. To demonstrate the targeted delivery of doxorubicin by SWNTs, we conjugated a cyclic RGD peptide on the terminal groups of PEG on SWNTs (Figure 5a), imparting a recognition moiety for integrin $\alpha_v\beta_3$ receptors up-regulated in

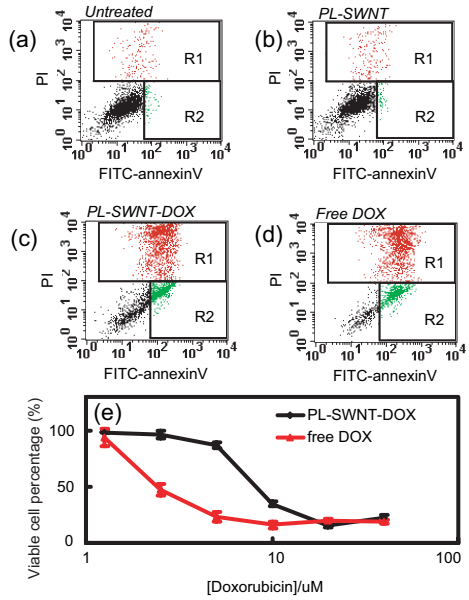

Figure 4. *In vitro* toxicity test of doxorubicin-loaded SWNTs. (a–d) Flow cytometry or flow-assisted cell sorting (FACS) data of U87MG cells treated by PL-SWNT (20 nM), free DOX (10 μM) and PL-SWNT-DOX ([SWNT] = 10 nM, [DOX] = 10 μM) for 24 h in solutions. The apoptotic cells were stained with FITC-annexin V (R2, green), while necrotic cells were stained with PI (R1, red). SWNT by itself (b) was nontoxic to cells, while DOX-loaded SWNTs induced significant apoptosis and cell death (c), as did free DOX (d). (e) Concentration-dependent cell survival curves of U87MG cells treated with PL-SWNT-DOX and free DOX, respectively. PL-SWNT-DOX showed a higher IC_{50} value (~8 μM) compared with that of free DOX (~2 μM).

a wide range of solid tumors.[22] Ultrahigh DOX loading was observed on PEG-RDG-functionalized SWNTs, without any loss of capacity due to the added RGD (Supporting Information, Figure S8). Enhanced doxorubicin delivery to integrin $\alpha_v\beta_3$-positive U87MG cells by RGD-conjugated SWNTs was indeed evidenced in various experiments, including confocal fluorescence imaging (Figure 5b). Much brighter DOX fluorescence signals were observed in integrin $\alpha_v\beta_3$-positive U87MG cells incubated with PL-SWNT-RGD-DOX, compared to those observed in cells treated by PL-SWNT-DOX without RGD (Figure 5b). This was attributed to a higher degree of cellular uptake of DOX when delivered by SWNTs conjugated with RGD peptide. The PL-SWNT-RGD-DOX showed an enhanced cell-killing effect toward U87MG cells, with a lower IC_{50} value (~3 μM) than that found prior to RGD conjugation (~8 μM), owing to specific RGD-integrin recognition and enhanced celluar uptake of the SWNT drug (Figure 5c). In contrast, for integrin $\alpha_v\beta_3$-negative MCF-7 cells, RGD conjugation onto SWNT-DOX gave no obvious enhancement in intracellular DOX delivery (Figure 5b). Concentration-dependent toxicity data showed that free DOX exhibited higher toxicity than both PL-SWNT-DOX and PL-SWNT-RGD-DOX to MCF cells (Figure 5d), suggesting that RGD conjugation to SWNTs afforded no enhancement in DOX delivery and destruction of integrin $\alpha_v\beta_3$-negative MCF cells. These results suggested the potential for selectively enhancing the toxicity of drugs to certain types of cells by using SWNTs conjugated with a targeting moiety as drug carriers.

Generality of Aromatic Molecules Noncovalently Binding onto PEGylated SWNTs. Finally, we found that molecular binding and absorption onto SWNTs is general to several types of aromatic molecules tested in this work, including a fluorescent dye molecule (fluorescein)[19] and another chemotherapy drug (daunorubicin), though the degree of loading on SWNTs and pH dependence varied for different molecules (Figure 6). The fluorescein derivative fluorescein cadaverine (FITC-NH_2, Molecular Probes) was loaded onto PEG-SWNTs with high efficiency at the isoelectric pH (p*I* ~ 6) of fluorescein. About 40 FITC molecules were loaded per 10 nm length of SWNTs (*vs* ~50 DOX per 10 nm of SWNTs loaded at pH 9). FITC was released from PL-SWNTs at high pH values due to the increased hydrophilicity resulting from deprotonation of the carboxylic acid group on the molecule. These results suggest that various types of small aromatic and hydrophobic molecules with low water solubility can be loaded onto the surface of SWNTs in

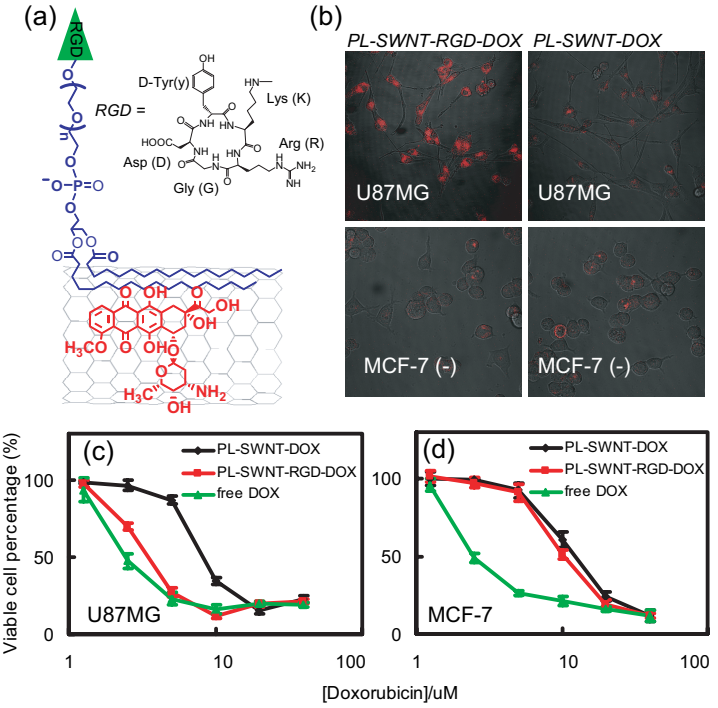

Figure 5. RGD peptide selectively enhances doxorubicin delivery by SWNTs and toxicity to integrin $\alpha_v\beta_3$-positive cells. (a) Schematic structure of PL-SWNT-RGD-DOX, *i.e.*, SWNTs functionalized with RGD at the termini of PEG and loaded with doxorubicin on the sidewall by π-stacking. (b) Confocal fluorescence images of integrin $\alpha_v\beta_3$-positive U87MG cells (top) and negative MCF-7 cells (bottom) treated with either PL-SWNT-DOX (right) or PL-SWNT-RGD-DOX (left). The concentration of DOX was 2 μM in all experiments. The U87MG cells incubated with PL-SWNT-RGD-DOX showed stronger DOX fluorescence in the cells than in the other three cases. (c,d) Concentration-dependent survival curves of U87MG cells (c) and MCF-7 cells (d) treated by various samples, as indicated. The viable cell percentage was measured by the MTS assay. PL-SWNT-DOX had a lower toxic effect than free DOX on both types of cells, while PL-SWNT-RGD-DOX exhibited increased toxicity to U87MG cells but not to MCF-7 cells.

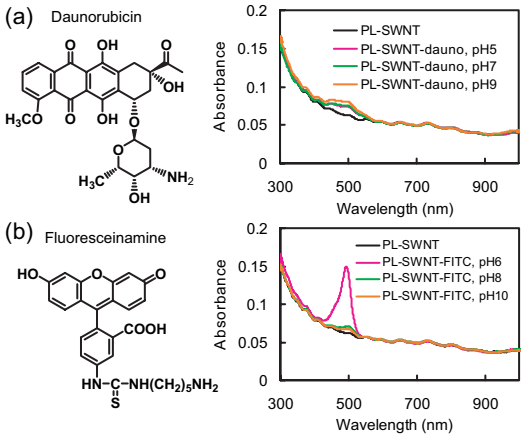

Figure 6. Supramolecular loading of other molecules on pre-PEGylated SWNTs. (a) UV–vis–NIR spectra of solutions of SWNTs and daunorubicin loaded at different pH values. (b) UV–vis–NIR absorbance spectra of SWNTs and fluorescein cadaverine (FITC-NH_2)-loaded SWNTs at different pH values. Daunorubicin exhibited pH-dependent loading behavior similar to that of doxorubicin, due to their similar molecular structures, while fluorescein cadaverine was loaded on SWNTs more strongly at lower pH (pH 6) than at higher pH. Note that the p*I* of fluoresceinamine is about 6.

the aqueous phase *via* noncovalent π-interaction. Such interaction is sufficiently strong to prevent rapid desorption in normal physiological conditions. Molecular release of the noncovalently bound molecules can be triggered by environmental changes such as pH or other external stimuli.

CONCLUSION

We have found that large areas still exist on various common functionalized SWNTs that retain high affinity for noncovalent binding of aromatic molecules *via* π-stacking. Consequently, prefunctionalized SWNTs can adsorb widely used aromatic molecules by simple mixing, forming "forest–scrub"-like assemblies on nanotubes with PEG extending into water to impart solubility and aromatic molecules densely populating the nanotube sidewalls. Our work establishes a novel, easy-to-make formulation of a SWNT–doxorubicin complex with extremely high drug loading efficiency. Counting the weight of PL-PEG coating, the SWNT–doxorubicin complex contains ~50–60 wt % of doxorubicin, which is remarkably higher than the ~8–10 wt % for conventional liposomes[23–25] and the latest reported dendrimer drug carriers.[26] The good stability of SWNT-DOX complexes in normal physiological buffer as well as serum, and fast drug release in acidic environments, are ideal properties for *in vivo* drug carriers. SWNT diameter-dependent drug binding and release behaviors allow multiple choices for drug carriers with different purposes. The functional groups outside the SWNT-DOX complexes are available for conjugation of other molecular ligands, including RGD peptide and potentially antibodies, which renders targeted delivery of drug. Multiple types of molecules with aromatic structure can π-stack onto prefunctionalized SWNTs. SWNTs are thus unique among high-surface-area materials, owing to extended polyaromatic structures favoring supramolecular chemistry with a wide range of important molecules. Combined with the *in vivo* tumor targeting of SWNTs achieved in mice,[12] our current work in drug loading opens up the door to *in vivo* cancer therapy using nanotubes. Thus, supramolecular chemistry on SWNTs could represent a new, exciting direction that may open up new opportunities in chemistry, biology, and medicine.

MATERIALS AND EXPERIMENTS

Starting Functionalized SWNT Materials. Noncovalent functionalized SWNTs were prepared as follows.[12,27] As-grown Hipco or laser-ablation SWNTs were sonicated in aqueous solution of PL-PEG5000-NH_2 (Sunbright DSPE-050-PA, NOF Corp.) at a ratio of 0.2 mg of SWNTs:0.5 mg of PL-PEG:1 mL of water for 1 h, followed by centrifugation at 24000*g* for 6 h, yielding well-suspended SWNTs (in the form of individual SWNTs and small bundles) in the supernatant. Unbound surfactant was thoroughly removed by repeated filtration through 100 kDa filters (Millipore) and resuspending SWNTs in water by sonication. The PL-PEG-functionalized SWNTs (denoted as PL-PEG-SWNT) were finally resuspended in phosphate-buffered saline (PBS).

Covalently functionalized SWNTs were prepared by refluxing 10 mg of as-grown Hipco SWNTs in 50 mL of 2.5 M nitric acid for 24 h. Acid was thoroughly removed by repeated filtration through 100 nm polycarbonate membrane (Millipore) and resuspension in water. PEGylation of carboxylic acid groups on the oxidized SWNTs (OXNT) was done by adding 1 mM poly(ethylene oxide), four-arm, amine-terminated (Aldrich, 565733), into the OXNT solution in the presence of 2 mM 1-ethyl-3-[3-dimethylaminopropyl]carbodiimide hydrochloride (Aldrich) under gentle sonication. After overnight reaction, unreacted reagents were removed by repeated filtration and resuspension of the covalently PEGylated SWNTs (denoted as PEG-OXNT).

Both the PL-PEG noncovalently functionalized and covalently PEGylated oxidized SWNTs were well solubilized and stable in water, PBS, and cell medium containing 10% fetal calf serum and full serum.[11,12] Atomic force microscopy was used to measure the diameter and length of the functionalized SWNTs after deposition on a Si substrate.

Supramolecular Assembly for Doxorubicin Loading onto Functionalized SWNTs. DOX loading onto PEG-functionalized SWNTs (PL-PEG-SWNT or PEG-OXNT) was done by simply mixing 1 mM DOX with the PEGylated SWNTs at a nanotube concentration of ~0.05 mg/mL (~300 nM) at various pH values overnight. Unbound excess DOX was removed by filtration through a 100 kDa filter and washed thoroughly with water (over 10 times) and PBS until the filtrate became free of reddish color (corresponding to free DOX). The formed complexes (denoted as PL-SWNT-DOX and OXNT-DOX) were then resuspended and stored at 4 °C.

UV–vis–NIR absorbance spectra of the SWNT-DOX complexes were measured by using a Cary-6000i spectrophotometer. The concentrations of SWNTs were determined by the absorbance at 808 nm with a molar extinction coefficient of $7.9 \times 10^6\ M \cdot cm^{-1}$ for PL-PEG-SWNT[10] and $4.0 \times 10^6\ M \cdot cm^{-1}$ for PEG-OXNT (Supporting Information) with an average tube length of ~200 nm. The concentration of DOX loaded onto SWNTs was measured by the absorbance peak at 490 nm (characteristic of DOX, after subtracting the absorbance of SWNTs at that wavelength) with a molar extinction coefficient of 1.05×10^5

$M \cdot cm^{-1}$. Note that thorough removal of free DOX was carried out by filtration prior to the measurement to accurately assess the amount of DOX loaded onto SWNTs. Fluorescence spectra were taken by using a Fluorolog-3 fluorimeter for free DOX and DOX bound to SWNTs at an excitation of 488 nm, to evaluate fluorescence quenching of DOX resulting from π-interaction with nanotubes.

Analysis of Molecular Release from Nanotubes. Solutions of PL-PEG-SWNT or PEG-OXNT loaded with DOX by the above procedure were allowed to stand for various times at room temperature at various pH values in carbonate buffer (pH 9), phosphate buffer (pH 7.4), or acetate buffer (pH 5.5) with the same ionic strength, adjusted by addition of sodium chloride. DOX molecules that detached from the SWNT surfaces over time were removed from solution by filtration through a 100 kDa filter. SWNTs were then resuspended in water for UV–vis–NIR measurement of the percentage of DOX retained (and thus released) on the nanotubes. To glean the temperature dependence of release, we kept solutions of PL-PEG-SWNT loaded with DOX (for both Hipco and laser-ablation nanotubes) for various times in PBS (pH 7.4) at 20, 40, 60, and 80 °C, respectively. The amount of released DOX was measured at different time points to obtain retained DOX on SWNTs *vs* time and calculate the retention half-life, $t_{1/2}$, at various temperatures (Supporting Information, Figure S7).

Loading of Doxorubicin onto RGD-PEG Functionalized SWNTs for Cellular Experiments. RGD peptide capable of selectively binding to integrin $\alpha_v\beta_3$ receptors on various cancer cells[28] was conjugated to PEGylated SWNTs as described previously.[12] Briefly, 1 mM sulfo-succinimidyl 4-*N*-maleimidomethylcyclohexane-1-carboxylate was mixed with ~0.05 mg/mL (~300 nM) PL-PEG-SWNT with amine groups at the PL-PEG termini (or OXNT with covalently attached PEG-NH_2) solutions at pH 7.4 for 2 h. Upon removal of excess reagents by fitration, the SWNTs were reacted overnight with 0.2 mM thiolated RGD[29] in the presence of 10 mM tris(2-carboxyethyl)phosphine hydrochloride at pH 7.4, completing RGD conjugation to the terminal amine groups of PEG chains on SWNTs. DOX loading was then done to the RGD-functionalized nanotubes (denoted as PL-SWNT-RGD-DOX) at the same conditions as for SWNTs without RGD, with similar loading efficiencies observed (Supporting Information, Figure S8).

MCF-7 breast cancer cells and U87MG human glioblastoma cancer cells (both from American Type Culture Collection) were cultured under standard conditions. Both MCF-7 and U87MG cells were incubated with PL-SWNT-DOX or PL-SWNT-RGD-DOX ([DOX] = 2 μM) for 1 h and washed by PBS twice before confocal imaging. Confocal fluorescence images were taken under a Zeiss LSM 510 microscope. Cells were incubated with series concentrations of PL-SWNT-DOX, PL-SWNT-RGD-DOX, and free DOX for 24 h before the cell viability test, which was performed by MTS assay with a CellTiter96 kit (Promega).

U87MG cells treated by SWNTs or drugs for 24 h were co-stained with propidium iodide (PI) and FITC-labeled annexin V before flow cytometry (Becton Dickinson) analysis. Necrotic cells were stained by PI, while apoptic cells were stained by FITC-annexin V.

Acknowledgment. This work was supported in part by a Ludwig Translational Research Grant at Stanford University, NIH-NCI CCNE-TR, and a Stanford Graduate Fellowship. We acknowledge Dr. Xiaoyuan Chen and Dr. Weibo Cai for kindly providing RGD peptide and for help in collecting the radiochemistry data available in the Supporting Information.

Supporting Information Available: Control experiments for DOX loading, stability of DOX-loaded SWNTs in serum, and measurement of DOX binding energy. This material is available free of charge *via* the Internet at http://pubs.acs.org.

REFERENCES AND NOTES

1. Hirsch, A. Functionalization of single-walled carbon nanotubes. *Angew. Chem., Int. Ed.* **2002**, *41*, 1853.
2. Sun, Y. P.; Fu, K. F.; Lin, Y.; Huang, W. J. Functionalized carbon nanotubes: Properties and applications. *Acc. Chem. Res.* **2002**, *35* (12), 1096.
3. Bahr, J. L.; Tour, J. M. Covalent chemistry of single-wall carbon nanotubes. *J. Mater. Chem.* **2002**, *12* (7), 1952.
4. Banerjee, S.; Hemraj-Benny, T.; Wong, S. S. Covalent surface chemistry of single-walled carbon nanotubes. *Adv. Mater.* **2005**, *17* (1), 17.
5. Britz, D. A.; Khlobystov, A. N. Noncovalent interactions of molecules with single walled carbon nanotubes. *Chem. Soc. Rev.* **2006**, *35* (7), 637.
6. Chen, R.; Zhang, Y.; Wang, D.; Dai, H. Non-covalent sidewall functionalization of single-walled carbon nanotubes for protein immobilization. *J. Am. Chem. Soc.* **2001**, *123* (16), 3838–3839.
7. Kam, N. W. S.; Liu, Z.; Dai, H. Functionalization of carbon nanotubes via cleavable disulfide bonds for efficient intracellular delivery of siRNA and potent gene silencing. *J. Am. Chem. Soc.* **2005**, *127* (36), 12492–12493.
8. Bianco, A.; Kostarelos, K.; Partidos, C. D.; Prato, M. Biomedical applications of functionalised carbon nanotubes. *Chem. Commun.* **2005**, *No. 5*, 571–577.
9. Cherukuri, P.; Bachilo, S. M.; Litovsky, S. H.; Weisman, R. B. Near-infrared fluorescence microscopy of single-walled carbon nanotubes in phagocytic cells. *J. Am. Chem. Soc.* **2004**, *126*, 15638–15639.
10. Kam, N. W. S.; O'Connell, M.; Wisdom, J. A.; Dai, H. J. Carbon nanotubes as multifunctional biological transporters and near-infrared agents for selective cancer cell destruction. *Proc. Natl. Acad. Sci. U.S.A.* **2005**, *102*, 11600–11605.
11. Liu, Z.; Winters, M.; Holodniy, M.; Dai, H. J. siRNA delivery into human T cells and primary cells with carbon-nanotube transporters. *Angew. Chem., Int. Ed.* **2007**, *46* (12), 2023–2027.
12. Liu, Z.; Cai, W. B.; He, L. N.; Nakayama, N.; Chen, K.; Sun, X. M.; Chen, X. Y.; Dai, H. J. In vivo biodistribution and highly efficient tumour targeting of carbon nanotubes in mice. *Nat. Nanotechnol.* **2007**, *2* (1), 47–52.
13. Dresselhaus, M. S.; Dai, H. Carbon nanotubes: Continued innovations and challenges. *MRS Bull.* **2004**, *29* (4), 237.
14. Dai, H. Carbon nanotubes: opportunities and challenges. *Surf. Sci.* **2002**, *500*, 218–241.
15. Chen, J.; Hammon, M. A.; Hu, H.; Chen, Y. S.; Rao, A. M.; Eklund, P. C.; Haddon, R. C. Solution properties of single walled carbon nanotubes. *Science* **1998**, *282*, 95–98.
16. Liu, J.; Rinzler, A. G.; Dai, H.; Hafner, J. H.; Bradley, R. K.; Boul, P. J.; Lu, A.; Iverson, T.; Shelimov, K.; Huffman, C. B.; Rodriguez-Macias, F.; Shon, Y.-S.; Lee, T. R.; Colbert, D. T.; Smalley, R. E. Fullerene pipes. *Science* **1998**, *280*, 1253–1256.
17. Zhao, B.; Hu, H.; Yu, A. P.; Perea, D.; Haddon, R. C. Synthesis and characterization of water soluble single-walled carbon nanotube graft copolymers. *J. Am. Chem. Soc.* **2005**, *127* (22), 8197.
18. Lehn, J. M. Supramolecular chemistry: receptors, catalysts, and carriers. *Science* **1985**, *227* (4689), 849.
19. Nakayama-Ratchford, N.; Bangsaruntip, S.; Sun, X. M.; Welsher, K.; Dai, H. J. Noncovalent functionalization of carbon nanotubes by fluorescein-polyethylene glycol: Supramolecular conjugates with pH-dependent absorbance and fluorescence. *J. Am. Chem. Soc.* **2007**, *129* (9), 2448–2449.
20. Li, Q. W.; Sun, B. Q.; Kinloch, I. A.; Zhi, D.; Sirringhaus, H.; Windle, A. H. Enhanced self-assembly, of pyridine-capped CdSe nanocrystals on individual single-walled carbon nanotubes. *Chem. Mater.* **2006**, *18* (1), 164–168.
21. Kam, N. W. S.; Liu, Z. A.; Dai, H. J. Carbon nanotubes as intracellular transporters for proteins and DNA: An investigation of the uptake mechanism and pathway. *Angew. Chem., Int. Ed.* **2006**, *45* (4), 577–581.
22. Mizejewski, G. J. Role of integrins in cancer: Survey of expression patterns. *Proc. Soc. Exper. Biol. Med.* **1999**, *222* (2), 124.
23. Storm, G.; ten Kate, M. T.; Working, P. K.; Bakker-

Woudenberg, I. A. J. M. Doxorubicin entrapped in sterically stabilized liposomes: Effects on bacterial blood clearance capacity of the mononuclear phagocyte system. *Clin. Cancer Res.* **1998**, *4* (1), 111–115.
24. Seymour, L. W.; Ulbrich, K.; Steyger, P. S.; Brereton, M.; Subr, V.; Strohalm, J.; Duncan, R. Tumor tropism and anticancer efficacy of polymer-based doxorubicin prodrugs in the treatment of subcutaneous murine B16F10 melanoma. *Br. J. Cancer* **1994**, *70* (4), 636–641.
25. Huang, S. K.; Mayhew, E.; Gilani, S.; Lasic, D. D.; Martin, F. J.; Papahadjopoulos, D. Pharmacokinetics and therapeutics of sterically stabilized liposomes in mice bearing C-26 colon-carcinoma. *Cancer Res.* **1992**, *52* (24), 6774–6781.
26. Lee, C. C.; Gillies, E. R.; Fox, M. E.; Guillaudeu, S. J.; Fréchet, J. M. J.; Dy, E. E.; Szoka, F. C. A single dose of doxorubicin-functionalized bow-tie dendrimer cures mice bearing C-26 colon carcinomas. *Proc. Natl. Acad. Sci. U.S.A.* **2006**, *103*, 16649–16654.
27. Kam, N. W. S.; Liu, Z.; Dai, H. J. Functionalization of carbon nanotubes via cleavable disulfide bonds for efficient intracellular delivery of siRNA and potent gene silencing. *J. Am. Chem. Soc.* **2005**, *127* (36), 12492–12493.
28. Chen, X.; Tohme, M.; Park, R.; Hou, Y.; Bading, J. R.; Conti, P. S. Micro-PET imaging of $\alpha_v\beta_3$-integrin expression with ^{18}F-labeled dimeric RGD peptide. *Mol. Imaging* **2004**, *3* (2), 96.
29. Cai, W. B.; Shin, D. W.; Chen, K.; Gheysens, O.; Cao, Q. Z.; Wang, S. X.; Gambhir, S. S.; Chen, X. Y. Peptide-labeled near-infrared quantum dots for imaging tumor vasculature in living subjects. *Nano Lett.* **2006**, *6* (4), 669.